Title

Structural changes upon magnetic ordering in magnetocaloric $AlFe_2B_2$

Journal

Applied Physics Letters, 116(21)

ISSN

0003-6951 1077-3118

Authors

Oey, Yuzki M

Bocarsly, Joshua D

Mann, Dallas

et al.

Publication Date

2020-05-26

DOI

10.1063/5.0007266

Peer reviewed

Structural changes upon magnetic ordering in magnetocaloric $AlFe_2B_2$

Yuzki M. Oey,[1, a)] Joshua D. Bocarsly,[1] Dallas Mann,[2] Emily E. Levin,[1] Michael Shatruk,[2] and Ram Seshadri[1]
[1)] *Materials Department and Materials Research Laboratory, University of California Santa Barbara, California 93106 United States*
[2)] *Department of Chemistry and Biochemistry, Florida State University 95 Chieftan Way, Tallahassee, Florida 32306, United States*

(Dated: 20 April 2020)

With a Curie temperature just above room temperature, $AlFe_2B_2$ is a useful magnetocaloric material composed of earth-abundant elements. We employ temperature-dependent high resolution synchrotron X-ray diffraction to establish with high certainly that the paramagnetic to ferromagnetic transition in $AlFe_2B_2$ is second order, showing no discontinuity in lattice parameters or cell volume. Nevertheless, the lattice parameters undergo anisotropic changes across the transition with distinct differences in the thermal expansion coefficients. While the a and b lattice parameters show positive thermal expansion, c shows negative thermal expansion. We link these changes to the respective interatomic distances to determine the contribution of magnetism to the anisotropic structural evolution. The work underpins the possible role of magnetostructural coupling in driving the magnetocaloric effect in $AlFe_2B_2$.

In recent years, magnetocaloric refrigeration has been proposed as an attractive alternative to traditional vapor-compression refrigeration as environmentally unsafe refrigerants can be avoided, and there is the promise of improved efficiency.[1,2] Magnetocaloric materials exhibit the magnetocaloric effect (MCE) and usually order ferromagnetically. When a magnetic field is applied to the material near its transition temperature, a paramagnetic to ferromagnetic transition is induced, causing the magnetic entropy to decrease significantly. If this magnetization is performed adiabatically, the temperature increases to conserve the overall entropy. Upon demagnetization, the temperature decreases. Thus, magnetocalorics with a magnetic phase transition near room temperature can be used as solid state magnetic refrigerants.[3] The gravimetric entropy change in the presence of a magnetic field under isothermal conditions, ΔS_M, is commonly used to characterize the magnitude of the MCE in a material.

Gadolinium is often considered the prototypical magnetocaloric material, with its large spin moment and Curie temperature near room temperature,[3] but for large-scale applications, more environmentally-friendly and earth-abundant materials are desired. Magnetically soft materials made with earth abundant elements with magnetic transitions near room temperature are therefore an attractive target in the search for practical magnetic refrigerants. While binary borides have high Curie temperatures,[4] more magnetically dilute borides can have transition temperatures closer to room temperature.[5,6] Because the transition temperatures of these materials directly affect their practicality, many studies have investigated how the Curie temperature can be tuned in intermetallic compounds.[7–12]

It is well known that magnetostructural coupling can lead to a giant MCE in materials with first-order magnetostructural phase transitions, such as transition seen in $Gd_5Si_2Ge_2$, which involves a change in magnetic state accompanied by a simultaneous change in crystal structure.[13,14] While the large entropy and temperature changes achievable with first-order magnetostructural transitions are desirable, such transitions present challenges for use in practical devices. First-order transitions show hysteresis, resulting in losses, and discontinuous structural transitions may lead to mechanical degradation and rate limitations while cycling. Therefore, it is of great interest to find materials with second-order phase transitions that nevertheless show a large MCE.

It is often assumed that the magnitude of the MCE observed at a continuous phase transition is only controlled by the saturation magnetization, while the role of magnetostructural coupling in these materials has frequently been overlooked. However, the Bean and Rodbell model,[16] which is frequently used to understand giant MCE materials, shows that magnetostructural coupling can also greatly enhance the MCE in materials with second-order transitions.[15] This model is supported by experimental results from systems such as $LaFe_{13-x}Si_x$[17] and $Mn_xFe_{1.95-x}P_{0.5}Si_{0.5}$,[18] where chemical tuning controls the strength of magnetostructural coupling within both first- and second-order regimes. Similarly, it was found that MnB displays much larger magnetoelastic coupling than FeB, and consequently shows a peak value of $-\Delta S_M$ that is three times larger.[4] A survey of magnetocalorics based on density functional theory calculations has established a broad correlation between magnetostructural coupling (approximated using magnetic deformation calculations) and MCE in materials with both first-order and continuous transitions.[11,12,19,20] This work made the prediction that $AlFe_2B_2$, among some other materials with strong magnetocaloric effects observed at continuous magnetic transitions, would display

[a)] Electronic mail: yoey@ucsb.edu

strong magnetostructural coupling when investigated experimentally.

$AlFe_2B_2$ was first isolated and its crystal structure solved by Jeitschko in 1969.[21] Much more recently the compound has been identified as a strong magnetocaloric comprising earth-abundant elements with a paramagnetic to ferromagnetic transition at 285 K.[5] This transition temperature increases to 308 K when $AlFe_2B_2$ is grown using Ga flux, possibly due to an off stoichiometry of Al:Fe,[22] and the maximum $-\Delta S_M$ for $H = 5$ T is around 8.0 J kg^{-1} K^{-1}.[5,23] For comparison, Gd, which serves as the benchmark magnetocaloric material, also shows peak $-\Delta S_M$ of around 8 J kg^{-1} K^{-1} at $H = 5$ T. The large MCE in Gd is generally attributed to its high saturation magnetization of 254 A m^2 kg^{-1}.[24] $AlFe_2B_2$, on the other hand, displays a saturation magnetization of just 80.6 A m^2 kg^{-1}. Although there was initial confusion about the nature of the transition in $AlFe_2B_2$ with a report of a first order transition,[25] more recent studies utilizing neutron diffraction and temperature– and field–dependent magnetization have suggested that $AlFe_2B_2$ actually undergoes a continuous transition.[26–29] Therefore, it is of interest to understand how $AlFe_2B_2$ achieves such a large MCE despite its modest saturation magnetization.

Here we show that a close look at the structural evolution of $AlFe_2B_2$ using high-resolution synchrotron X-ray diffraction data acquired at temperatures spanning the Curie temperature reveals that while $AlFe_2B_2$ does not exhibit any discontinuities or structure-type changes across its magnetic transition temperature, it does display pronounced magnetoelastic effects. The magnetic transition is accompanied by anisotropic evolution of the a, b, and c lattice parameters as well as the atomic positions. Our findings for $AlFe_2B_2$ are supported by DFT calculations that show that magnetostructural coupling, and not just saturation magnetization, plays a key role in inducing a large MCE at second-order magnetic transitions. Other promising magnetocalorics displaying second-order phase transitions may also show magnetostructural coupling if they are studied more carefully using high-resolution synchrotron or neutron diffraction.

Samples of $AlFe_2B_2$ were prepared using Ga flux as previously reported.[5] A Quantum Design Physical Property Measurement System (PPMS) Dynacool with a vibrating sample magnetometer (VSM) was used to take temperature–dependent magnetization data at $H = 0.2$ T between 5 K and 375 K. Field–dependent magnetization data were acquired at a temperature of 5 K in a field between $H = -5$ T and 5 T. To determine the magnetic entropy change as a function of applied field, $\Delta S_M(H,T)$ was obtained from the appropriate Maxwell relation, using M *vs.* T measurements taken by sweeping temperature at fixed magnetic fields between $H = 0.1$ T and 5 T and data were analyzed using the `magentro.py` code.[30] High-resolution synchrotron powder X-ray diffraction data were acquired at the Argonne National Laboratory, Advanced Photon Source (APS) on

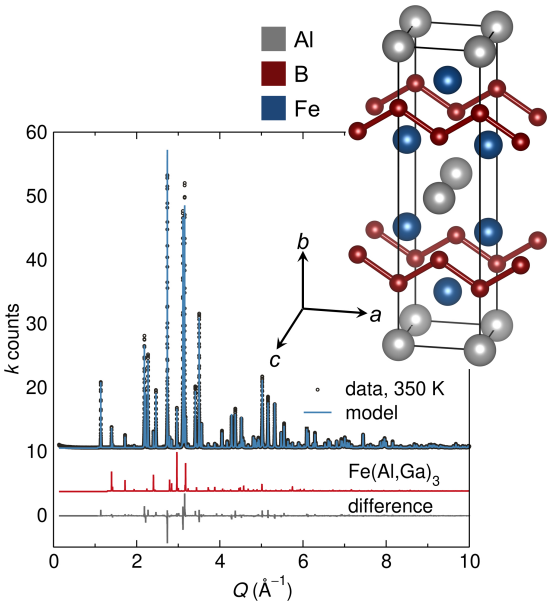

FIG. 1. High-resolution synchrotron X-ray diffraction data acquired at $T = 350$ K fit using Rietveld refinement with the two phases $AlFe_2B_2$ (space group $Cmmm$, #65) and $Fe(Al,Ga)_3$ (6.20(3) wt.%, space group $P4_2/mnm$, #136). The crystal structure of $AlFe_2B_2$ displayed as an inset consists of 1-D chains of B atoms running along the a axis separating Fe atoms. Al are at the corners and are C-centered. The $Cmmm$ structure of $AlFe_2B_2$ at 350 K: $a = 2.93392(1)$ Å; $b = 11.05318(2)$ Å; $c = 2.87466(1)$ Å. Al at $2a$, (0,0,0); Fe at $4j$, (0,0.35397(1),0.5), and B at $4i$, (0,0.2066(1),0). Parentheses on the last significant figure indicate calculated uncertainty.

beamline 11-BM with an average wavelength of $\lambda = 0.414581$ Å. Data at 200 K and 350 K were collected between $Q = 0.1$ Å^{-1} to 12 Å^{-1}. Temperature-dependent diffraction patterns were collected in the range $Q = 1.00$ Å^{-1} to 4.75 Å^{-1} every 2.3 K as the sample was cooled from 336 K to 282 K, and every 0.5 K between 312 K and 300 K through the magnetic transition. Topas Academic[31] was used to refine the patterns using both sequential and parametric refinement.[32] Crystal structures were visualized using VESTA.[33]

Rietveld refinement of the synchrotron data acquired at 350 K is shown in Fig. 1. Due to the anisotropic nature of $AlFe_2B_2$,[34] the patterns were fit using the Stephens peak-shape function for an orthorhombic phase.[35] The main phase is orthorhombic $Cmmm$ $AlFe_2B_2$ as expected.[5] A tetragonal $P4_2/mnm$ secondary phase $Fe(Ga,Al)_3$[36] that was not detected on a laboratory X-ray diffractometer is observed in this synchrotron pattern as 6.20(3) wt.% of the sample, with Ga being incorporated from the flux. The refined composition of this phase is $FeGa_{1.828(8)}Al_{1.172(8)}$ with lattice parameters $a = b = 6.25621(2)$ Å and $c = 6.48051(4)$ Å. Because this secondary phase exists as a constant weight percent through all of the scans, we assume that it does not affect the structural transition that we observe in the main

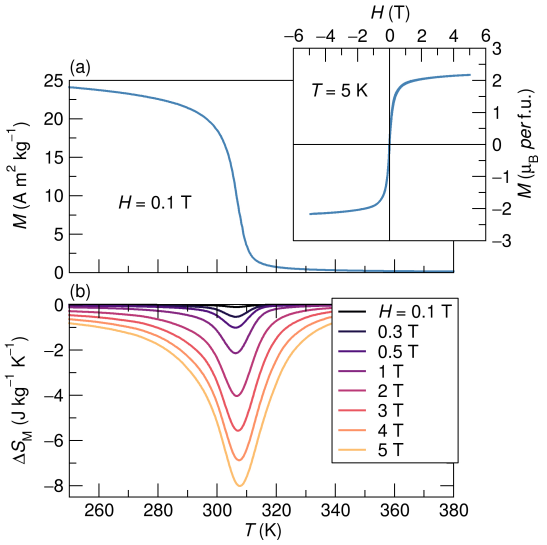

FIG. 2. (a) Temperature dependent magnetization of $AlFe_2B_2$ acquired under a field of H = 0.1 T. Field dependent magnetization taken at T = 5 K is shown in the inset. The adjusted saturation magnetization value for only $AlFe_2B_2$ at T = 5 K and H = 5 T is 80.6 A m^2 kg^{-1} (emu g^{-1}). (b) At a field of H = 5 T, $-\Delta S_M$ has a maximum value of 8.0 J kg^{-1} K^{-1}.

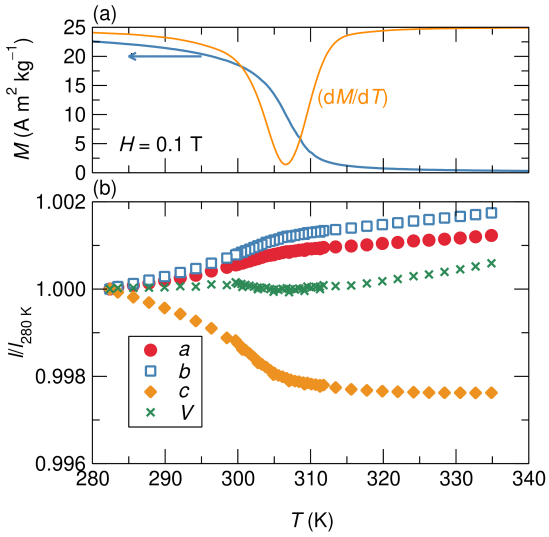

FIG. 3. (a) Temperature–dependent magnetization taken at H = 0.1 T with its respective derivative (peaking at 308 K) is compared with the (b) evolution of scaled lattice parameters a, b, and c, and unit cell volume as a function of temperature. The values in (b) are normalized by their respective values at T = 280 K. a and b display positive thermal expansion in the temperature range displayed, while c displays large negative thermal expansion.

phase $AlFe_2B_2$. Moreover, $Fe(Ga, Al)_3$ is not magnetic,[36] so it does not contribute to the magnetism observed for this sample. The $AlFe_2B_2$ structure (inset of Fig. 1) consists of B atoms spaced 1.75 Å apart arranged in 1-D zigzag chains along the a axis, with Fe atoms between these chains. The caption of Fig. 1 lists key structural details from the refinement of the T = 350 K data.

Figure 2(a) displays M *vs.* T under a constant field H = 0.1 T and confirms the reported ferromagnetic ordering at T_C = 308 K.[5] The inset of this figure shows M *vs.* H at T = 5 K. The saturation moment is 75.6 A m^{2}kg^{-1} for the sample, and with 6.20(3) wt.% non-magnetic secondary phase, the saturation moment for $AlFe_2B_2$ is 80.6 A m^2 kg^{-1} (2.31 μ_B f.u.$^{-1}$). This yields a magnetic moment of 1.16 μ_B Fe^{-1}, comparable to reported DFT calculated moments of 1.25 μ_B Fe^{-1} to 1.32 μ_B Fe^{-1}.[5,19] Figure 2(b) displays the evolution of the magnetic entropy change under different applied maximum magnetic fields. A large $-\Delta S_M$ value of 8.0 J kg^{-1} K^{-1} was observed under H = 5 T, thereby confirming the previously reported magnetocaloric properties of $AlFe_2B_2$.[5] The relatively low saturation magnetization and yet significant ΔS_M indicate that saturation magnetization is not the only driving factor for the MCE in $AlFe_2B_2$.

To investigate how structure evolves as a function of temperature, parametric Rietveld refinements were performed on variable-temperature synchrotron X-ray diffraction data. Fig. 3(b) displays normalized lattice parameters as a function of temperature, and a and b show positive thermal expansion while c shows considerable negative thermal expansion. All three lattice parameters show non-linear changes without any discontinuities, indicative of a second order phase transition. The sharpest change in these parameters occurs at the magnetic transition temperature, where the lattice parameters either increase or decrease by about 0.1% to 0.2% between 310 K and 280 K. The unit cell volume shows overall slight thermal expansion, but right below the T_C between 300 K and 308 K there is a slight contraction, leading to very little overall change. This is reminiscent of the Invar effect in which there is almost zero volume change with temperature after the onset of magnetization.[37] Although a 0.1% to 0.2% change in lattice parameter may seem small, these changes are many times stronger than the magnetostriction commonly observed in ferromagnetic materials,[38] including Gd.[39] These changes are, however, comparable to those seen in MnB, which has been found to derive a strong MCE from its magnetostructural coupling.[4]

It is interesting to compare these lattice parameter changes to the results of the DFT magnetic deformation study reported previously.[19] In the previous study, DFT structural optimizations with and without spin polarization were performed to estimate the effect that magnetism plays on the structure. For $AlFe_2B_2$, upon the introduction of spin polarization, the a, b, and c lattice parameters changed by –0.8%, –2.6%, and 5.6%, respectively. The changes upon magnetic ordering in the experimental lattice parameters are far smaller (as usual), but mirror these signs and relative magnitudes remarkably well, with the largest increase in lattice parameter seen in the c axis and smaller negative changes seen in

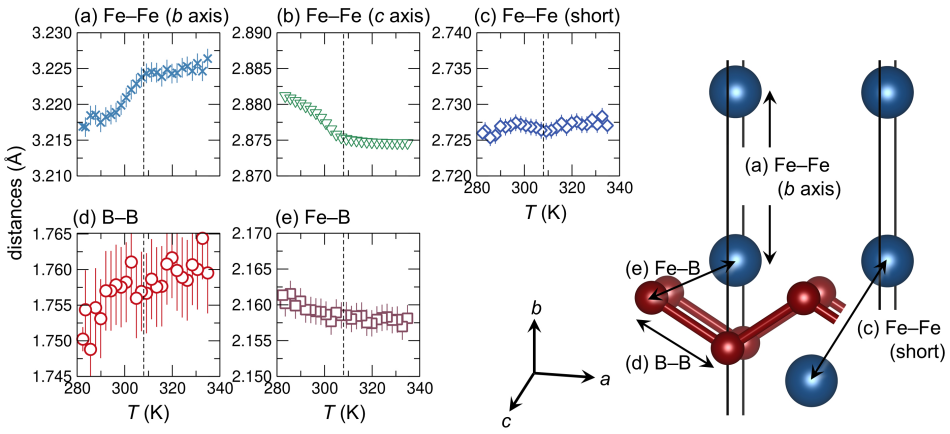

FIG. 4. Evolution of atom–atom distances across the Curie temperature of $T_C = 308$ K (indicated as a dashed vertical line). (a) The Fe–Fe distances along the b axis show positive thermal expansion until the transition temperature, whereupon the rate of expansion displays a distinct decrease. (b) Between unit cells along the c direction, Fe atoms are bonded and show the greatest change in the slope. (c) The shortest Fe–Fe distance remains largely constant over this temperature range, suggesting that the competing lattice expansion in the b direction and contraction in the c direction almost balance out for these pairs of atoms. Neither the (d) B–B bonds nor the (e) closest Fe–B distances change very much. For clarity, all of the panels (a) through (e) have the same ordinate range of 0.02 Å; the distances discussed in the panels are related to the crystal structure on the right.

the b and a axes. This is interesting because non-spin-polarized DFT is not, in general, a good approximation for the high-temperature paramagnetic state as it does not consider the effect of local magnetic moments. The strong correspondence between experiment and calculation seen here may be due to the fact that the magnetism in $AlFe_2B_2$ shows substantially itinerant character.[27]

Interatomic distances (Fig. 4) show concomitant anisotropic evolution with temperature due to a combination of the lattice parameters and internal atomic coordinates. Most notably, the Fe–Fe distance along the b axis between adjacent unit cells has pronounced positive thermal expansion from about 3.217 Å to 3.226 Å (Fig. 4a). However, this expansion is not as smooth as the b parameter shown in Fig. 3, suggesting that the cell may not be uniformly expanding. Meanwhile, the Fe-Fe distance along the c axis, which is equivalent to the c lattice parameter, shows the opposite effect (Fig. 4b). The shortest Fe–Fe contact, which lies in the ab plane, shows only very small changes, but an anomaly at the magnetic transition temperature can be clearly resolved (Fig. 4c). The B–B bonds connecting adjacent B atoms show the largest fractional change across the Curie temperature, with positive thermal expansion from about 1.75 Å to 1.76 Å (around 0.5%) between 280 K and 340 K (Fig. 4d), while the shortest Fe–B interaction shows slight negative thermal expansion, indicative of the competing forces of the a parameter positive expansion and c parameter negative expansion (Fig. 4e). Based on these results, we can conclude that magnetic order is accompanied by a strengthening of the B–B bonding and the Fe–Fe bonding along the b axis at the expense of weakening Fe–Fe bonding along the c axis and the Fe–B bonding.

Despite the modest saturation magnetization in $AlFe_2B_2$, the material shows a significant magnetocaloric effect comparable to that of Gd metal. Here, we propose that this effect is driven by magnetostructural coupling, which we observe through high-resolution temperature-dependent synchrotron studies. Given that $AlFe_2B_2$ has quite a large $-\Delta S_M$ and pronounced magnetostructural coupling, but shows no hysteresis, it may sit close to a tricritical point between first- and second-order magnetic transitions.[40] In this way, $AlFe_2B_2$ derives enhanced magnetocaloric properties from magnetostructural interaction without the practical downsides associated with first-order transitions. Our results suggest that the large MCE seen in other materials with continuous transitions may also be attributed to magnetostructural coupling instead of purely to saturation magnetization. Furthermore, strategies to control the strength of magnetostructural coupling in materials with continuous transitions, such as by chemical substitutions, are expected to be powerful tools to optimize the magnetocaloric effect.

Supplementary Material

See supplementary material for the cif file of $AlFe_2B_2$ from synchrotron X-ray diffraction data taken at 350 K.

Acknowledgments

The work at UC Santa Barbara was supported by the National Science Foundation (NSF) through DMR 1710638. The work at FSU was supported by the NSF through DMR 1905499. The research reported here made use of shared facilities of the NSF Materials Research Science and Engineering Center at UC Santa Barbara DMR 1720256; a member of the Materials Research Facilities Network (www.mrfn.org). Use of the Advanced Photon Source at Argonne National Laboratory was supported by the U.S. Department of Energy, Office of Sci-

ence, Office of Basic Energy Sciences, under Contract No. DE-AC02-06CH11357. YMO and JDB have been supported by the National Science Foundation Graduate Research Fellowship Program under Grant No. DGE-1650114.

References

[1] V. Franco, J. Blázquez, B. Ingale, and A. Conde, "The magnetocaloric effect and magnetic refrigeration near room temperature: materials and models," Annu. Rev. Mater. Res. **42**, 305–342 (2012).

[2] V. Franco, J. Blázquez, J. Ipus, J. Law, L. Moreno-Ramírez, and A. Conde, "Magnetocaloric effect: From materials research to refrigeration devices," Prog. Mater. Sci. **93**, 112–232 (2018).

[3] G. Brown, "Magnetic heat pumping near room temperature," J. Appl. Phys. **47**, 3673–3680 (1976).

[4] J. D. Bocarsly, E. E. Levin, S. A. Humphrey, T. Faske, W. Donner, S. D. Wilson, and R. Seshadri, "Magnetostructural coupling drives magnetocaloric behavior: The case of MnB versus FeB," Chem. Mater. **31**, 4873–4881 (2019).

[5] X. Tan, P. Chai, C. M. Thompson, and M. Shatruk, "Magnetocaloric effect in $AlFe_2B_2$: toward magnetic refrigerants from earth-abundant elements," J. Am. Chem. Soc. **135**, 9553–9557 (2013).

[6] P. Chai, S. A. Stoian, X. Tan, P. A. Dube, and M. Shatruk, "Investigation of magnetic properties and electronic structure of layered-structure borides AlT_2B_2 (T = Fe, Mn, Cr) and $AlFe_{2-x}Mn_xB_2$," J. Solid State Chem. **224**, 52–61 (2015).

[7] S. Hirt, F. Yuan, Y. Mozharivskyj, and H. Hillebrecht, "$AlFe_{2-x}Co_xB_2$ (x = 0–0.30): T_C Tuning through Co substitution for a promising magnetocaloric material realized by spark plasma sintering," Inorg. Chem. **55**, 9677–9684 (2016).

[8] R. Barua, B. Lejeune, B. Jensen, L. Ke, R. McCallum, M. Kramer, and L. Lewis, "Enhanced room-temperature magnetocaloric effect and tunable magnetic response in Ga-and Ge-substituted $AlFe_2B_2$," J. Alloys Compd. **777**, 1030–1038 (2019).

[9] M. Fries, Z. Gercsi, S. Ener, K. P. Skokov, and O. Gutfleisch, "Magnetic, magnetocaloric and structural properties of manganese based monoborides doped with iron and cobalt– A candidate for thermomagnetic generators," Acta Mater. **113**, 213–220 (2016).

[10] E. E. Levin, J. D. Bocarsly, K. E. Wyckoff, T. M. Pollock, and R. Seshadri, "Tuning the magnetocaloric response in half-Heusler/Heusler $MnNi_{1+x}Sb$ solid solutions," Phys. Rev. Mater. **1**, 075003 (2017).

[11] E. E. Levin, J. D. Bocarsly, J. H. Grebenkemper, R. Issa, S. D. Wilson, T. M. Pollock, and R. Seshadri, "Structural coupling and magnetic tuning in $Mn_{2-x}Co_xP$ magnetocalorics for thermomagnetic power generation," APL Mater. (2019), accepted.

[12] J. A. Cooley, M. K. Horton, E. E. Levin, S. H. Lapidus, K. A. Persson, and R. Seshadri, "From waste-heat recovery to refrigeration: Compositional tuning of magnetocaloric $Mn_{1+x}Sb$," Chem. Mater. **32**, 1243–1249 (2020).

[13] V. K. Pecharsky and K. A. Gschneidner, Jr., "Giant Magnetocaloric Effect in $Gd_5(Si_2Ge_2)$," Phys. Rev. Lett. **78**, 4494–4497 (1997).

[14] W. Choe, V. K. Pecharsky, A. O. Pecharsky, K. A. Gschneidner, V. G. Young, and G. J. Miller, "Making and breaking covalent bonds across the magnetic transition in the giant magnetocaloric material $Ge_5(Si_2Ge_2)$," Phys. Rev. Lett. **84**, 4617–4620 (2000).

[15] A. Davarpanah, J. H. Belo, V. S. Amaral, and J. S. Amaral, "On the optimization of magneto-volume coupling for practical applied field magnetic refrigeration," Phys. status solidi **256**, 1800419 (2019).

[16] C. P. Bean and D. S. Rodbell, "Magnetic disorder as a first-order phase transformation," Phys. Rev. **126**, 104–115 (1962).

[17] V. Franco, J. Y. Law, A. Conde, V. Brabander, D. Y. Karpenkov, I. Radulov, K. Skokov, and O. Gutfleisch, "Predicting the tricritical point composition of a series of LaFeSi magnetocaloric alloys via universal scaling," J. Phys. D. Appl. Phys. **50**, 414004 (2017).

[18] N. H. Dung, L. Zhang, Z. Ou, and E. Brück, "From first-order magneto-elastic to magneto-structural transition in $(Mn,Fe)_{1.95}P_{0.50}Si_{0.50}$ compounds," App. Phys. Lett. **99**, 092511 (2011).

[19] J. D. Bocarsly, E. E. Levin, C. A. Garcia, K. Schwennicke, S. D. Wilson, and R. Seshadri, "A simple computational proxy for screening magnetocaloric compounds," Chem. Mater. **29**, 1613–1622 (2017).

[20] C. A. C. Garcia, J. D. Bocarsly, and R. Seshadri, "Computational screening of magnetocaloric alloys," Phys. Rev. Mater. **4**, 024402 (2020).

[21] W. Jeitschko, "The crystal structure of Fe_2AlB_2," Acta Crystallogr. B **25**, 163–165 (1969).

[22] B. Lejeune, D. L. Schlagel, B. Jensen, T. A. Lograsso, M. J. Kramer, and L. Lewis, "Effects of Al and Fe solubility on the magnetofunctional properties of $AlFe_2B_2$," Phys. Rev. Mater. **3**, 094411 (2019).

[23] A. El Boukili, N. Tahiri, E. Salmani, H. Ez-Zahraouy, M. Hamedoun, A. Benyoussef, M. Balli, and O. Mounkachi, "Magnetocaloric and cooling properties of the intermetallic compound $AlFe_2B_2$ in an AMR cycle system," Intermetallics **104**, 84–89 (2019).

[24] J. Elliott, S. Legvold, and F. Spedding, "Some magnetic properties of gadolinium metal," Phys. Rev. **91**, 28 (1953).

[25] L. Lewis, R. Barua, and B. Lejeune, "Developing magnetofunctionality: Coupled structural and magnetic phase transition in $AlFe_2B_2$," J. Alloys Compd. **650**, 482–488 (2015).

[26] J. Cedervall, M. S. Andersson, T. Sarkar, E. K. Delczeg-Czirjak, L. Bergqvist, T. C. Hansen, P. Beran, P. Nordblad, and M. Sahlberg, "Magnetic structure of the magnetocaloric compound$AlFe_2B_2$," J. Alloys Compd. **664**, 784–791 (2016).

[27] T. N. Lamichhane, L. Xiang, Q. Lin, T. Pandey, D. S. Parker, T.-H. Kim, L. Zhou, M. J. Kramer, S. L. Bud'ko, and P. C. Canfield, "Magnetic properties of single crystalline itinerant ferromagnet $AlFe_2B_2$," Phys. Rev. Mater. **2**, 084408 (2018).

[28] B. T. Lejeune, X. Du, R. Barua, J.-C. Zhao, and L. H. Lewis, "Anisotropic thermal conductivity of magnetocaloric $AlFe_2B_2$," Acta Mater. **1**, 150–154 (2018).

[29] T. Ali, M. Khan, E. Ahmed, and A. Ali, "Phase analysis of $AlFe_2B_2$ by synchrotron X-ray diffraction, magnetic and Mössbauer studies," Prog. Nat. Sci. Mater. **27**, 251–256 (2017).

[30] J. D. Bocarsly, R. F. Need, R. Seshadri, and S. D. Wilson, "Magnetoentropic signatures of skyrmionic phase behavior in FeGe," Phys. Rev. B **97**, 100404 (2018).

[31] A. A. Coelho, "TOPAS and TOPAS-Academic: An optimization program integrating computer algebra and crystallographic objects written in C++," J. Appl. Crystallogr. **51**, 210–218 (2018).

[32] G. W. Stinton and J. S. Evans, "Parametric Rietveld refinement," J. Appl. Crystallogr. **40**, 87–95 (2007).

[33] K. Momma and F. Izumi, "VESTA 3 for three-dimensional visualization of crystal, volumetric and morphology data," J. Appl. Crystallogr. **44**, 1272–1276 (2011).

[34] R. Barua, B. Lejeune, L. Ke, G. Hadjipanayis, E. M. Levin, R. McCallum, M. Kramer, and L. Lewis, "Anisotropic magnetocaloric response in $AlFe_2B_2$," J. Alloys Compd. **745**, 505–512 (2018).

[35] P. W. Stephens, "Phenomenological model of anisotropic peak broadening in powder diffraction," J. Appl. Crystallogr. **32**, 281–289 (1999).

[36] D. Mondal, C. Kamal, S. Banik, A. Bhakar, A. Kak, G. Das, V. Reddy, A. Chakrabarti, and T. Ganguli, "Structural and electronic properties of $Fe(Al_xGa_{1-x})_3$ system," J. Appl. Phys. **120**, 165102 (2016).

[37] M. van Schilfgaarde, I. Abrikosov, and B. Johansson, "Origin of the Invar effect in iron–nickel alloys," Nature **400**, 46–49 (1999).

[38] J. A. Cooley, J. D. Bocarsly, E. C. Schueller, E. E. Levin, E. E. Rodriguez, A. Huq, S. H. Lapidus, S. D. Wilson, and R. Seshadri, "Evolution of non-collinear magnetism in magnetocaloric MnPtGa," Phys. Rev. Mater. (2020), accepted.

[39] K. P. Belov, Y. V. Ergin, and A. A. Ped'ko, "Magnetostriction of a Gadolinium single crystal," J. Exptl. Theor. Phys. **22**, 414–419 (1966).

[40] I. Takeuchi and K. Sandeman, "Solid-state cooling with caloric materials," Phys. Today **68**, 48 (2015).